NASA Technical Memorandum 83482

Analysis of an Externally Radially Cracked Ring Segment Subject to Three-Point Radial Loading

B. Gross, J. E. Srawley, and J. L. Shannon, Jr.
Lewis Research Center
Cleveland, Ohio

(NASA-TM-83482) ANALYSIS OF AN EXTERNALLY RADIALLY CRACKED RING SEG. NT SUBJECT TC THREE-POINT RADIAL LCADING (NASA) 12 p HC A02/MF A01 CSCL 20K

N83-35413

Unclas

G3/39 42101

Prepared for the
Sixteenth Symposium on Fracture Mechanics
cosponsored by Battelle Columbus Laboratories and the ASTM
Columbus, Ohio, August 15-17, 1983

NASA

ANALYSIS OF AN EXTERNALLY RADIALLY CRACKED RING SEGMENT SUBJECT TO THREE-POINT RADIAL LOADING

B. Gross, J. E. Srawley, and J. L. Shannon, Jr.
National Aeronautics and Space Administration
Lewis Research Center
Cleveland, Ohio 44135

E-1804

ABSTRACT

The boundary collocation method was used to generate Mode I stress intensity and crack mouth opening displacement coefficients for externally radially cracked ring segments subjected to three point radial loading. Numerical results were obtained for ring segment outer-to-inner radius ratios (R_o/R_i) ranging from 1.10 to 2.50 and crack length to segment width ratios (a/W) ranging from 0.1 to 0.8. Stress intensity and crack mouth displacement coefficients were found to depend on the ratios R_o/R_i and a/W as well as the included angle between the directions of the reaction forces.

SYMBOLS

a	crack length
B	ring segment thickness
E	Young's modulus
E'	$= E/(1 - \nu^2)$ for plane strain, = E for plane stress
K	mode-I stress intensity factor
M	crack plane moment at nominal neutral axis position: $M = P \tan \theta_1 (R_i + R_o - a)/4$
$\overline{n}$	unit outward normal vector along the collocation boundaries
P	applied load
R_i	ring segment inner radius
R_o	ring segment outer radius
V	total crack mouth opening displacement
W	ring segment width $= R_o - R_i$
x,y	Cartesian coordinates
R,θ	polar coordinates

θ_1 angle defining ring segment half-span (reaction load included half-angle)

θ_z angle defining ring segment boundary BC

ν Poisson's ratio

$\chi(R,\theta)$ stress function

INTRODUCTION

The arc-tension specimen is currently standardized as an alternate test specimen in ASTM Standard Test Method E399-81 for use in making plane strain fracture toughness measurements on sections sliced from tubular products. The specimen loses its utility as the ratio of outer-to-inner radii approaches unity, whereby it no longer has room to accommodate loading pin holes. For such cases, there is a need for an arc-bend specimen which requires no loading pin holes.

The authors have recently published a boundary collocation analysis for the mode-I crack stress intensity factor and mouth opening displacement coefficients for an internally radially cracked ring segment in three-point bending (1). The analysis was made to provide crack field solutions to be used in standardizing the arc-bend specimen as an alternate fracture toughness specimen in ASTM Standard Test Method E399-81. The results have been compared to an earlier finite element analysis by Jones (2). In contrast to Jones, the authors showed a functional dependence of the coefficients on the included angle between the directions of the reaction forces. This dependence agrees with the trend of maximum tensile stress determined by Nelson, et al., (3) for an uncracked bar subjected to three-point bending forces.

Cracks may originate from either the inner or outer wall of tubular products. Therefore, as an extension of the authors' work on the internally radially cracked ring segment, the present analysis is made on an externally radially cracked ring segment in three-point bending.

ORIGINAL PAGE IS
OF POOR QUALITY

ANALYTICAL APPROACH

The boundary collocation method of analysis used here has been described in detail by Gross and Mendelson (4) and by Gross and Srawley (5). Homogeneity, isotropy, and plane elasto-static conditions are assumed. Loading of the segment is by three-point concentrated radial forces as shown in figure 1.

Boundary conditions must be satisfied by the stress function and its derivative normal to the boundaries AB, BC, and CD (refer to fig. 1). Those along the radial boundary BC are obtained from a known stress function solution for the bending of an uncracked curved beam by radial forces (6):

along BC

$$\chi(R, \theta_z) = \frac{P \sin(\theta_1 - \theta_z)}{\left[\left(R_i^2 - R_o^2\right) + \left(R_i^2 + R_o^2\right) \ln\left(\frac{R_o}{R_i}\right)\right] 2 \cos \theta_1}$$

$$\times \left[\frac{R^3}{2} - \frac{R_i^2 R_o^2}{2R} - R\left(\left(R_i^2 + R_o^2\right) \ln\left(\frac{R}{R_o}\right) + \left(\frac{R_o^2 - R_i^2}{2}\right)\right)\right]$$

$$\left.\frac{\partial \chi}{\partial n}\right|_{R,\theta_z} = \frac{-P \cos(\theta_1 - \theta_z)}{\left[\left(R_i^2 - R_o^2\right) + \left(R_i^2 + R_o^2\right) \ln\left(\frac{R_o}{R_i}\right)\right] 2 \cos \theta_1}$$

$$\times \left[\frac{R^2}{2} - \frac{R_i^2 R_o^2}{2R^2} - \left(R_i^2 + R_o^2\right) \ln\left(\frac{R}{R_o}\right) - \left(\frac{R_o^2 - R_i^2}{2}\right)\right]$$

From the boundary requirements along arc boundaries AB and CD that the normal and shear stresses be zero, the stress function variation compatible with that along boundary BC at points B and C is obtained:

along arc AB $\quad \chi(R_o,\theta) = 0$

$$\left.\frac{\partial \chi}{\partial n}\right|_{R_o,\theta} = 0$$

along arc CD $\quad \chi(R_i,\theta) = \dfrac{PR_i \sin(\theta_1 - \theta)}{2 \cos \theta_1}$

$$\left.\frac{\partial \chi}{\partial n}\right|_{R_i,\theta} = \frac{-P \sin(\theta_1 - \theta)}{2 \cos \theta_1}$$

The Williams stress function (7) for the crack singularity is matched to the values of the stress function and its normal derivative along the boundary AB-BC-CD.

The boundary collocation was applied to sixty boundary stations using an overdetermined system of equations (4). Seven R_o/R_i ratios in the range 1.10 to 2.50 were treated; and for each, eight a/W ratios ranging from 0.1 to 0.8. For each combination of R_o/R_i and a/W ratios, seven to ten ring segment included arc angles $2\theta_1$ were examined. For a given arc angle $2\theta_1$, the angle θ_z defines the boundary BC. Convergence is assumed when variations in the parameter θ_z by about ± 20 percent produces no significant change in the mode-I stress intensity factor and crack mouth opening displacement coefficients.

RESULTS AND DISCUSSION

A complete tabulation of the results is given in reference 8 in the form of dimensionless mode-I crack stress intensity factor and mouth opening displacement coefficients. Selected results are shown graphically in figures 2 through 4 along with companion results for the internally cracked segment from reference 1. The extreme combinations of R_o/R_i and a/W analyzed are represented in figures 2 and 3. Results for $a/W = 0.5$, corresponding to the standardized crack relative length in ASTM Standard Test Method E399-81 are shown in figure 4 for the two smallest R_o/R_i ratios. These small R_o/R_i ratios are characteristic of tubular cross sections too thin to accommodate tension loading pin holes and therefore would require testing in the arc-bend specimen configuration.

In all cases, both coefficients are found to depend on the ratios R_o/R_i and a/W as well as the included angle $2\theta_1$ between the direction of the reaction forces. For given values of a/W, $2\theta_1$, and R_o/R_i, as the radius of curvature increases, so does the stress intensity factor coefficient, approaching in the limit those of a straight beam. The mouth opening displacement coefficient, as normalized here, is on the other hand only weakly dependent on curvature. Increasing a/W has the expected effect of markedly increasing both coefficients.

Dependence of the coefficients on the included angle $2\theta_1$ is modest but by no means negligible and needs to be taken into consideration in the design of a testing arrangement. The dependence fades at included angles greater than 90°. It is unlikely that a standardized arc-bend specimen would feature included angles less than 90°, thereby minimizing the angle dependence. For $a/W = 0.5$, $2\theta_1 > 90°$, and $R_o/R_i = 1.10$, for both the internally and externally cracked ring segments the variation of the normalized coefficients is less than 1.2 percent. Similarly for $R_o/R_i = 1.25$ the variation is less than 3 percent.

For a given load, crack relative length, and reaction load included angle, the moment arm is greater for the internally cracked segment than for the external crack. Therefore the coefficients for the internally cracked segment are greater than those for the externally cracked segment, but both vary about the same with $2\theta_1$.

REFERENCES

1. Gross, B. and Srawley, J. E., "Analysis of an Internally Radially Cracked Ring Segment Subject to Three-Point Radial Loading," Journal of Testing and Evaluation, Vol. 11, No. 6, Nov. 1983.

2. Jones, A. T., "Fracture Toughness Testing With Sections of Cylinders," Engineering Fracture Mechanics, Vol. 6, No. 4, Dec. 1974, pp. 653-662.

3. Nelson, C. W., Ancker, C. J., Jr., and Wu, Ning-Gau, "The Stresses in a Flat Curved Bar Due to Concentrated Radial Loads," Journal of Applied Mechanics, Vol. 19, No. 4, Dec. 1952, pp. 529-536.

4. Gross, B. and Mendelson, A., "Plane Elastostatic Analysis of V-Notched Plates," International Journal of Fracture Mechanics, Vol. 8, No. 3, Sept. 1972, pp. 267-276.

5. Gross, B. and Srawley, J. E., "Analysis of Radially Cracked Ring Segments Subject to Forces and Couples," in Developments in Fracture Mechanics Test Methods Standardization, ASTM STP 632, 1977, pp. 39-56.

6. Fung, Y. C., Foundations of Solid Mechanics, Prentice-Hall, Edgewood Cliffs, NJ, 1965.

7. Williams, M. L., "Stress Singularities Resulting from Various Boundary Conditions in Angular Corners of Plates in Extension," Journal of Applied Mechanics, Vol. 19, No. 4, Dec. 1952, pp. 526-528.

8. Gross, B. and Srawley, J. E., "Stress Intensity and Displacement Coefficients for a Radially Cracked Ring Segments Subjected to Three-Point Bending," NASA Report TM-83059, Mar. 1983.

ORIGINAL PAGE IS
OF POOR QUALITY

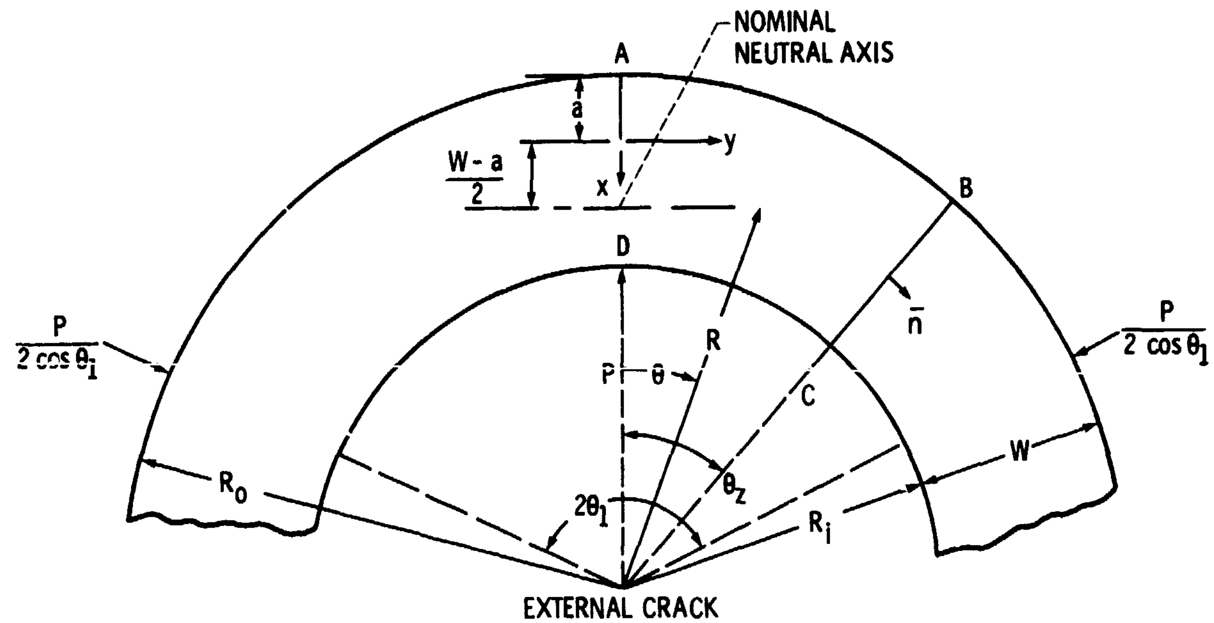

Figure 1. - Ring segment model and notation.

ORIGINAL PAGE IS
OF POOR QUALITY

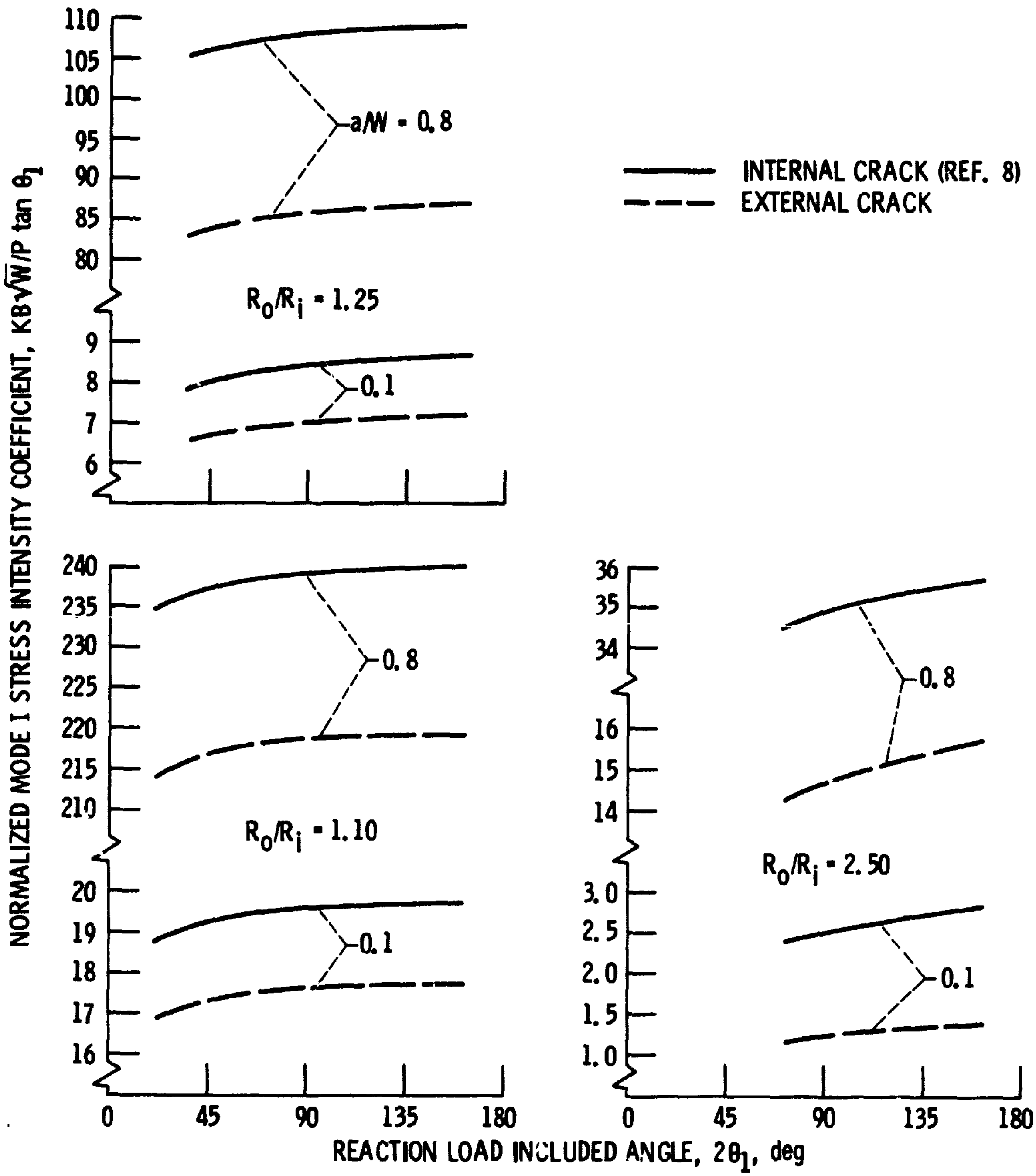

Figure 2. - Variation of the normalized mode-I stress intensity factor coefficient with reaction load included angle.

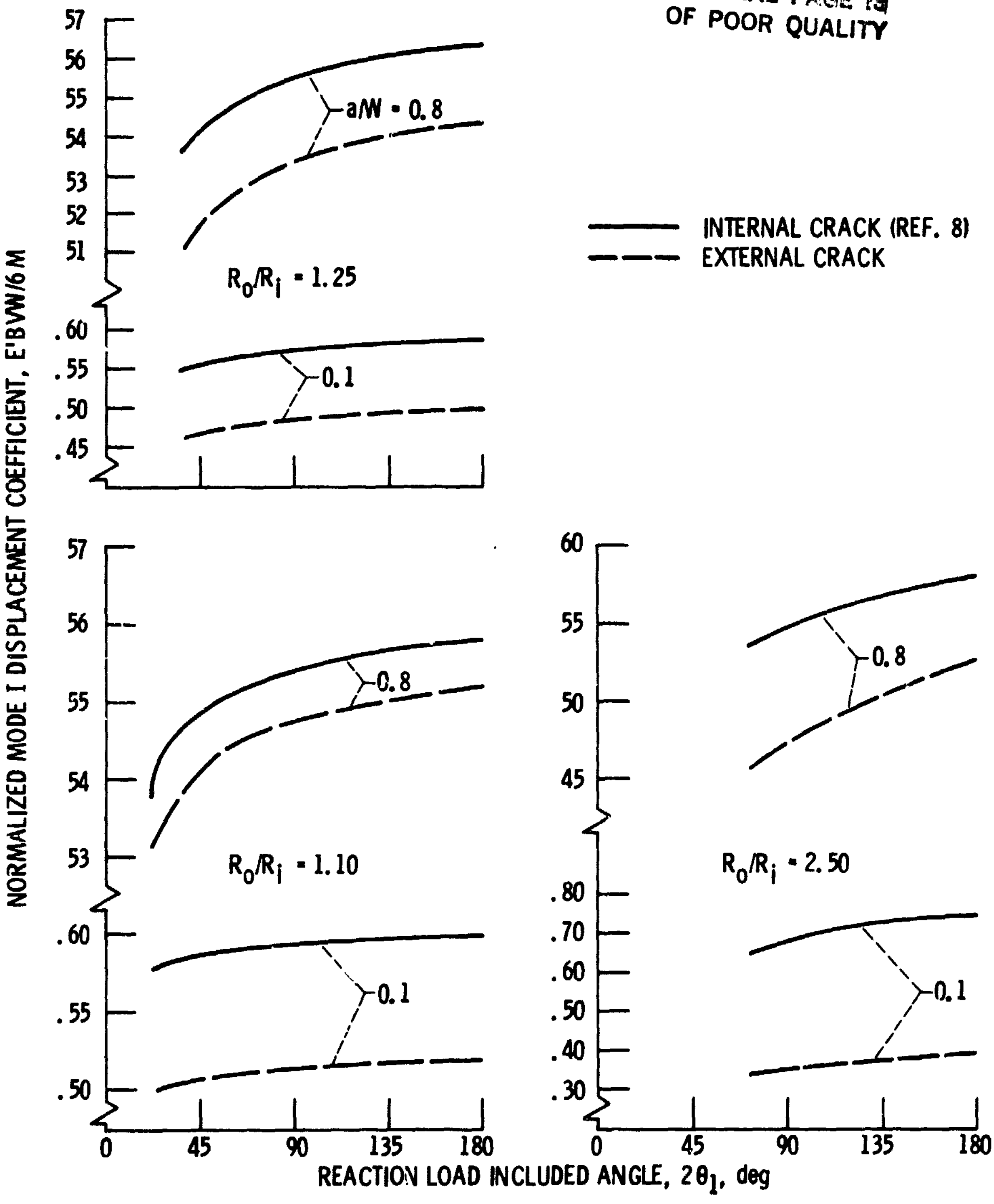

Figure 3. - Variation of the normalized mode-I crack mouth opening displacement coefficient with reaction load included angle.

ORIGINAL PAGE IS
OF POOR QUALITY

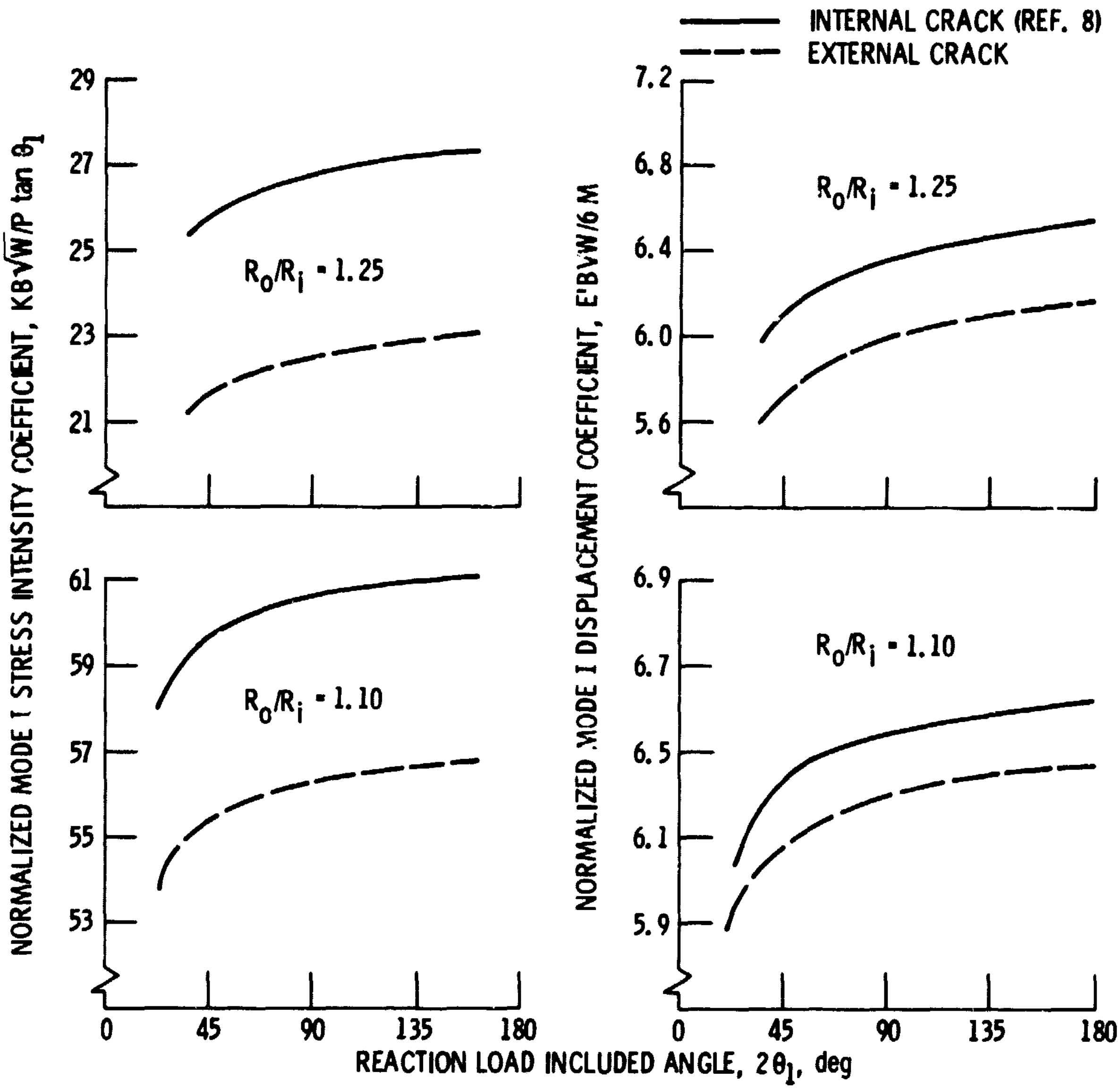

Figure 4. - Variation of the normalized Mode-I stress intensity and displacement coefficients with reaction load included angle for relative crack length a/W = 0.5.